Thermal conductivity and diffusivity estimations for shallow geothermal systems

Jon Busby

British Geological Survey, Keyworth, Nottingham, NG12 5GG, UK.

Email jpbu@bgs.ac.uk

Abstract

Horizontal closed loop ground collectors for ground source heat pumps are located within the soil and the top of the underlying, superficial deposits. Estimating thermal properties for this zone is difficult as it is heterogeneous and is subject to seasonal water content variations. Soil thermal diffusivity values have been calculated at 56 sites using temperature data from United Kingdom Met Office weather stations. The technique utilises the decrease in amplitude and increase in phase shift with depth, of a transmitted heat pulse in the ground, the magnitudes of which are determined by thermal diffusivity. The weather stations are located throughout Great Britain and incorporate different soil types. The apparent thermal diffusivities derived from seasonal temperature cycles spanning several years generates, seasonally averaged, site specific estimates that can be considered alongside diffusivity values determined in the laboratory or obtained by point measurements using field needle probes. Associated thermal conductivities have been estimated from the thermal diffusivities from knowledge of soil texture. Median thermal conductivities for the sand, loam and clay soil types have been estimated as 1.56, 1.15 and 1.81 W m^{-1} K^{-1} respectively with corresponding thermal diffusivities of 0.9961, 0.7173 and 1.0295 x 10^{-6} m^2 s^{-1}.

Shallow ground source heat collector loops often comprise straight pipes or coiled pipes (commonly referred to as slinkies™) that are laid horizontally along the base of a trench, or coiled pipes that are inserted vertically in a slit trench (Banks 2012). The suggested depth of the trenches varies, but GSHPA (2014) recommend 0.8-1.5 m below ground level and Banks (2012) indicates 1.2-2 m. These trenches are therefore located within the soil and the top of the underlying, superficial deposits. This unconsolidated geological material is often referred to as the parent material of the soil and is a geological deposit over, and within which, a soil develops (Lawley 2008). Soils can be categorised as sand, silt, clay and loam (or combinations of these) where a loam is composed of approximately equal amounts of sand, silt and clay. The length of the collector loop depends on many factors, but the ground's thermal properties (thermal conductivity and thermal diffusivity) will either need to be estimated or measured (e.g., GSHPA 2014, IGSHPA 1996; VDI 2001; Banks 2012; Preene & Powrie 2009; Curtis et al. 2013) to ensure adequate sizing of the loop.

There is a paucity of data on soil thermal properties required for the sizing of horizontal collector loops that is compounded by their seasonal dependence. A field method for estimating soil thermal properties is given by IGSHPA (1989). Many quoted, measured soil thermal properties are based on laboratory measurements (e.g. Clarke et al. 2008). These often use bulk soil samples that are bagged in the field, in which case the in-situ consolidation is lost and is recreated in the laboratory. However, this will alter the bulk density which is an important parameter in determining the thermal properties (e.g. Kersten 1949). Alternatively, field samples can be taken with a corer that incorporates a liner to preserve the natural texture and moisture, before transfer to the laboratory for thermal properties testing. For borehole based, vertical systems, a thermal response test can be performed to measure in-situ, bulk, thermal conductivity (e.g. Banks et al. 2013), but there is at present no equivalent for horizontal systems. Thermal conductivities at a point on the ground can be measured with a needle probe (Campbell et al., 1991, Bilskie et al., 1998, Bristow et al., 1993). Field probes are mounted on a long handle so that they can be inserted into the base of auger holes to over a metre depth. The probe generates a constant heat output and is a transient technique that monitors the increase of temperature with time. The determined thermal conductivity is only representative of a small cylindrical volume around the probe and errors can result from the contact between the probe and the soil. King et al.

(2012) have indicated that a minimum of 12 – 16 measurements should be taken at a site with a field probe to produce a representative geometric mean thermal conductivity. However, such values are still only valid for a particular point in time as near surface thermal properties are affected by the seasonal variation in soil moisture. As an example of this variation, Gonzalez et al. (2012) quote a 37% increase at 0.75 m depth and a 23% increase in soil thermal conductivity at 1 m depth between dry summer and wet winter conditions for a loamy sand (average composition; clay: 2.4%; Silt: 33.2%; Sand: 64.4%) that developed over a superficial deposit of sand and gravel.

Apparent thermal diffusivity can be determined from soil temperature measurements and has been widely reported (e.g. Kappelmeyer and Haenel, 1974; Adams et al., 1976; Horton et al., 1983; Verhoef et al., 1996; Gao et al., 2009). The technique utilises the decrease in amplitude and delay in temperature change (phase shift) with depth of a transmitted heat signal applied to the ground surface, the magnitudes of which are determined by thermal diffusivity. If the heat signal is periodic, i.e. the diurnal or seasonal temperature cycle, and it is assumed that the heat transfer is governed by the one-dimensional heat conduction equation; six different methods for calculating thermal diffusivity can be defined (Horton et al. 1983). Adams et al. (1976) and Horton et al. (1983) found that some of these methods gave erratic results. This may be partly due to using temperature measurements from the upper 10 cm of the soil, a zone where heat transfer is unlikely to be purely by conduction and to too few temperature measurements which do not adequately describe the periodic signal.

This paper explores the calculation of soil thermal properties by utilising the database of British meteorological soil temperature measurements taken at multiple depths to a maximum depth of 1 m. Thermal diffusivity is calculated directly from the depth distributed soil temperatures and thermal conductivity is estimated from the diffusivity measurements with the addition of assumed parameters based on soil texture. The soil temperature measurements are widely dispersed covering many soil types and occupy the depth range of a horizontal ground collector loop. The calculated thermal properties are annual averages rather than a single seasonal value taken at a point in time. Although specifically incorporating British datasets the results and conclusions are applicable to shallow ground source heat in general.

Methodology

Data selection and preparation

Soil temperature data are collected and archived by the UK Met Office and are made available for academic purposes via the British Atmospheric Data Centre (http://badc.nerc.ac.uk/home). The data are recorded at 09:00 each day to the nearest 0.1 ºC at depths of 5, 10, 20, 30, 50 and 100 cm, although not all depths are covered at each station and some temperature depth records may be discontinuous. Temperature data from two depths are required for a thermal diffusivity determination. In general, these sites are on level ground with no trees, buildings or steep ground nearby (Met Office 2010). Stations with automatic systems use platinum resistance thermometers where the head of the thermometer is inserted into the undisturbed soil on the vertical wall on the side of a trench which is then back filled. However, this is impractical for the 100 cm measurement where the thermometer is suspended inside a tube with its tip at the appropriate depth. At manned climate stations, soil temperature is measured by mercury-in-glass thermometers read by the observer. Thermometers for the 10 cm measurement have a right angled bend in the tube so that the bulb may be buried in the soil at the required depth and the scale exposed horizontally above the surface for easy reading. At depth, they are suspended inside tubes and are housed in an extra protective glass sheath and have their bulb set in wax to slow their response while being withdrawn and read by the observer (Met Office 2010).

For this study, time series temperature data from 65 Met Office weather stations have been used, as shown in Figure 1 and listed in Table 1. The data cover the period 2000-2010 and utilise depth intervals of 50-100 cm and 30-100 cm, although a small number of determinations were made from the depth ranges 30-50 cm and 10-30 cm when no data were available from 100 cm depth. Figure 2 displays a typical soil temperature record for 3 years from the meteorological station at Woburn with daily temperature readings at 30 cm depth (black lines) and 100 cm depth (grey lines). It has been suggested (Hinkel 1997) that the amplitudes of the fundamental frequency of the annual cycle can be approximated from the minimum and maximum temperature readings. However, as can be seen in Figure 2, the raw data display daily temperature fluctuations which can be considered as diurnal noise on the seasonal cycle. Hence a function of the form;

$$Y = b0 + b1\cos(yX) + c1\sin(yX) \tag{1}$$

has been fitted to the data (see the smooth lines in Figure 2) from which the annual amplitudes and the phase shift can be extracted. Such an approach smoothes the temperature data resulting in a seasonal temperature cycle. In some cases, a full 11 years temperature record was available, but often, due to either extensive data drop outs or discontinuous data caused by malfunction of the measuring sensors, the record was shorter. The minimum record length used in this study was two complete years.

Thermal diffusivity estimation

The theoretical development for estimating thermal diffusivity from two vertically separated soil temperature measurements is well known (Kappelmeyer & Haenel 1974; Adams et al. 1976; Horton et al. 1983). It can be shown that for vertical, conductive heat transfer where the ground surface temperature changes are periodic, the thermal diffusivity, α, can be calculated from;

$$\propto = \frac{\omega}{2}\left[\frac{z_2 - z_1}{\ln\frac{A_1}{A_2}}\right]^2 \tag{2}$$

where z_1 and z_2 are the depths of the temperature measurements, A_1 and A_2 are the amplitudes of the periodic temperature at z_1 and z_2 and ω is the fundamental angular frequency of the periodic temperature. This is referred to as the amplitude equation. Similarly α can be calculated from;

$$\propto = \frac{1}{2\omega}\left[\frac{z_2 - z_1}{\delta t}\right]^2 \tag{3}$$

where δt is the phase difference between temperature variations at the two depths z_1 and z_2. This is referred to as the phase equation. The amplitudes A_1 and A_2 and the phase difference δt are shown in Figure 2.

These two equations can be combined to give the relationship between amplitude damping and phase delay, i.e.

$$\ln\frac{A_2}{A_1} = -\omega\delta t \tag{4}$$

Any deviation from this relationship is an indication of nonconductive behaviour within the zone of measurement of the amplitudes and phase shift (Koo & Song 2008; Koo et al. 2003) and can be used to quality check any calculated thermal diffusivities.

Thermal conductivity estimation

Thermal conductivity can be estimated from thermal diffusivity via the relation;

$$\lambda = \alpha S_{vc} \tag{5}$$

where λ is thermal conductivity (W m^{-1} K^{-1}), α is thermal diffusivity (m^2 s^{-1}) and S_{vc} is specific heat capacity by volume (J K^{-1} m^3). Specific heat capacity by volume is often referred to as thermal capacity to distinguish it from specific heat capacity by mass (Waples & Waples 2004a). Soil samples were not available from each of the Met Office weather stations, and so it was necessary to estimate thermal capacity.

Waples & Waples (2004b) give a relation for the thermal capacity of a mixture of solids and liquids as the weighted average of the thermal capacities of the component solids and liquids, i.e.

$$S_{vc(soil)} = S_{vc(mineral)}(1 - \phi) + S_{vc(water)}MC + S_{vc(air)}(\phi - MC) \quad (6)$$

where ϕ is the fractional porosity, MC is the fractional water content and $S_{vc(mineral)}$ is the thermal capacity of the mineral component of the soil. Since the thermal capacity of air ($S_{vc(air)}$) is very small (1.29 x 10^{-9} J K^{-1} m^{3}) the final term in the above equation can be ignored.

Waples & Waples (2004a) compiled an extensive database of heat capacities for the inorganic minerals. For low and medium density inorganic minerals ($\rho \leq 4000$ kg m^{-3}) they derived a predictive relationship between mineral density and thermal capacity at 20 ºC, i.e.

$$S_{vc(mineral)} = 1.0263e^{0.2697\rho} \quad (7)$$

where mineral density (ρ) is g cm^{-3} and thermal capacity is J K^{-1} cm^{-3}.

Therefore, the parameters required for the estimation of thermal capacity are the bulk and particle densities, porosity and moisture content and these have been estimated from the assessed soil texture at each Met Office station site. Due to the lack of detailed soil mapping, an indication of soil texture can be obtained from the BGS Parent Material Map. Typically, the parent material is the first recognisably geological deposit encountered when excavating beneath the pedological soil layer. This data includes a general pedological classification of soil texture from measured soil samples overlying the parent material (Lawley 2008) based on a UK classification of soil texture designed by the National Soil Research Institute (Hodgson 1997).

Based on the available soil texture data, approximate bulk densities were obtained from http://pedosphere.ca/resources/bulkdensity/worktable_us.cfm which has adopted the method of Saxton et al. (1986) and is based on the U.S. soil texture triangle. Soil porosities were taken from standard texts (e.g. Dingman 2002; IAEA 2008) and range from 0.55% for a clay soil to 0.39% for a sand soil. Water contents are also standard values, ranging from 20% for a clay soil to 8% for a sand soil. The particle density of the mineral component of the soil was calculated from the bulk density and porosity via the relation,

$$\rho_{(particle)} = \frac{\rho_{(bulk)}}{(1-\emptyset)} \tag{8}$$

All of these estimated parameters are listed in Table 2 and descriptions of the soil textures are given in Table 3.

From the estimated particle densities (Table 2), estimated thermal capacities for the mineral component of the soil have been determined from equation (7). The thermal capacity of the soil was then calculated from equation (6) and, finally, these estimated soil thermal capacities were multiplied by the thermal diffusivity determinations (equation 5) to generate a set of estimated thermal conductivities.

Results

Apparent thermal diffusivity

Thermal diffusivities were calculated for the depth intervals 50-100 cm (30 determinations), 30-100 cm (38 determinations), 30-50 cm (3 determinations) and 10-30 cm (2 determinations). For every thermal diffusivity determination there is an amplitude and phase shift derived diffusivity. These are sometimes divergent and this has been attributed to heat transfer that is not one-dimensional (vertical) conductive flow (Koo & Song, 2008). Figure 3 shows a plot of the amplitude damping against the phase delay for all 73 thermal diffusivity determinations. Also shown in Figure 3 is equation (4) (bold line), along which heat transfer is solely by one-dimensional conductive flow, and two dashed lines that represent a deviation from equation (4) by ± 4%. Amplitude and phase thermal diffusivities that fall between the dashed lines have been taken as representing one-dimensional conductive heat transfer and the final thermal diffusivity is the mean of the amplitude and phase values. A total of 13 (18%) thermal diffusivity determinations were therefore rejected, comprising 3 (10%) at 50-100 cm depth, 9 (24%) at 30-100 cm depth and 1 (50%) at 10-30 cm depth. A listing of the accepted, 60 thermal diffusivity values from 56 Met Office weather stations, are shown in Table 2.

There is a wide range of derived thermal diffusivity values ranging from 0.3517 to 2.4691 x 10^{-6} m^2 s^{-1}. The rejection rate of 24% for the 30-100 cm depth measurements is double that for 50-100 cm depth, indicating that non-conductive heat flow is more prevalent at shallow depth. At four sites (Mylnefield, Rothamsted, Buxton and Halesowen), accepted thermal diffusivities were calculated at both 50-100 cm and 30-100 cm depths. Of these only one (Rothamsted) gave a different result at the two depths. Since these determinations represent seasonally averaged values it is likely that the main factor influencing the thermal diffusivity is soil texture.

Thermal conductivity

Estimated thermal conductivities were calculated from the 60 thermal diffusivity values and range from 0.54 to 3.81 W m^{-1} K^{-1} with the minimum and maximum thermal conductivities coinciding with the equivalent thermal diffusivities. As with thermal diffusivity, for the four sites with determinations at two depths, only 1 (Rothamsted) gave a different result at the two depths. A key step in generating the thermal conductivities has been the estimation of thermal capacities. In order to compare with some published results, the soil thermal capacities have been converted to soil specific heats by the relation;

$$S_{vc} = S_c \, \rho \tag{9}$$

where S_c is specific heat capacity (J kg^{-1} K^{-1}) and ρ is the density (kg m^{-3}) and these are shown in Table 2. Adjepong (1997) published the results of specific heat capacity measurements on 3 soil types (clay, sand and sandy loam) with water contents varied from 0 to 25%. For each of these soil types, the specific heats from Table 2 have been averaged and are compared to the results of Adjepong (1997) in Table 4. There is good agreement between the two sets of data with clay soil specific heat around 1500 J kg^{-1} K^{-1} and sandy soils around 1000 J kg^{-1} K^{-1}, indicating that the estimates are reasonable.

Discussion

The approach presented here utilised soil temperature data within the installation depth range of a horizontal ground collector loop to determine, seasonally averaged, thermal diffusivity values. Estimates of thermal conductivity have then been derived from these diffusivity data and from soil texture data. The values demonstrate the range of soil thermal conductivities and diffusivities that might be expected at the sites investigated. The lowest thermal conductivity of 0.54 W m^{-1} K^{-1} is from the Mylnefield site (src_id = 181), which is a sandy soil and so indicates well drained, dry conditions. The highest value of 3.81 W m^{-1} K^{-1} from Penmaen (src_id = 1256) is also a sandy site and so is indicative of saturated conditions. Based on the dominant soil type, thermal diffusivities and conductivities have been plotted on box whisker plots and are shown in Figures 4 and 5. The dominant soil types are sand, loam, silt and clay, but only one site was classed as silt. The soil texture classes of 'ALL' and 'L_C_S' were not included as they do not fit into a single dominant soil type. The two plots show the same trends illustrating that the estimated parameters applied to the thermal conductivity calculation have not had a dominant effect. As might be expected, the sand soils have a greater range of thermal properties reflecting the greater range of water saturation. The clay soil type has the highest conductivity and diffusivity (median) values and loam has the lowest. The median thermal conductivities for the sand, loam and clay soil types are 1.56, 1.15 and 1.81 W m^{-1} K^{-1} respectively (and the corresponding median thermal diffusivities are 0.9961, 0.7173 and 1.0295 x 10^{-6} m^2 s^{-1}).

The results derived here can be compared against those obtained from other available approaches. King et al. (2012) report the results from a thermal needle probe used on two sites. At the first site (80 m x 40 m), described as silty clay or clayey silt of variable moisture content, measured minimum, maximum and geometric mean thermal conductivities were 0.43, 1.93 and 1.22 W m^{-1} K^{-1} respectively. At the second site (110 m x 30 m), described as damp or waterlogged clayey sand and sandy clay, measured corresponding thermal conductivities were 1.09, 2.5 and 1.65 W m^{-1} K^{-1} respectively. It was unclear if the range in these data resulted from variations in soil texture across the sites or changes in soil moisture content. The second site is a combination of sand and clay soil types. From Figure 4 the mean of the sand and clay median thermal conductivities is 1.69 W m^{-1} K^{-1}, in close agreement with the geometric mean value of King et al. (2012).

Modelling schemes are often employed to estimate thermal conductivity when laboratory measurements of soil physical properties are unavailable. One such modelling approach has recently been implemented by Bertermann et al. (2014). The approach is based on Kersten (1949) and Dehner (2007) and requires the water content and bulk density of the soil as the main input parameters. In their study, water content was estimated from the humidity of the region (estimated from mean annual rainfall and mean annual temperature) and soil texture; whilst bulk density was estimated from soil texture. Applying the water content calculations of Bertermann et al. (2014) to this study, but using the soil textures and bulk densities in Table 2, a set of modelled thermal conductivities were generated. These were plotted against the thermal conductivities derived using the soil temperature measurements from Table 2 and are shown in Figure 6. It can be seen that there is no correlation between these two sets of thermal conductivities. This occurs because the primary input parameter for the method of Bertermann et al. (2014) was the soil texture, whereas in this study it was the thermal diffusivity. Hence, the method of Bertermann et al. (2014) may be better suited for regionalised values of thermal conductivity, whilst the method here is more site specific reflecting variability in soil texture and water content.

Conclusions

In this study, soil temperature data, collected routinely by the UK Met Office were successfully applied to calculate soil thermal diffusivity values at 56 stations throughout Great Britain, of different soil types. Using determinations from seasonal temperature cycles spanning several years, results in thermal diffusivities that are seasonally averaged, site specific estimates derived for the depth range within which horizontal closed loop ground collectors are buried. They are therefore another source of thermal diffusivity data that can be considered alongside values determined in the laboratory or obtained by point measurements using field needle probes. Associated thermal conductivities were estimated using soil texture data from the BGS Parent Material map. Median thermal conductivities for the sand, loam and clay soil types have been estimated as 1.56, 1.15 and 1.81 W m^{-1} K^{-1} respectively with corresponding thermal diffusivities of 0.9961, 0.7173 and 1.0295 x 10^{-6} m^2 s^{-1}. Thermal properties calculated using this approach can provide valuable inputs for assessing and calibrating modelled data sets. The approach also includes an effective screening method to identify and remove measurements that are affected by nonconductive heat transfer processes, hence increasing the confidence in/reliability of the results.

Acknowledgements

This paper is published by permission of the Executive Director of the British Geological Survey (NERC). The UK Met Office is thanked for making available the soil temperature data held in the Met Office Database – MIDAS and made available through the British Atmospheric Data Centre (BADC).

References

ADAMS, W. M., WATTS, G. & MASON G. 1976. Estimation of thermal diffusivity from field observations of temperature as a function of time and depth. *American Mineralogist*, **61**, 560-568.

ADJEPONG, S. K. 1997. Investigation of the variation of the specific heat capacity of three texture types of soil with moisture content. *Journal of Applied Science and Technology*, **2**, 7-12.

Banks, D. 2012. An Introduction to Thermogeology: Ground source heating and cooling. 2nd Edition. Wiley- Blackwell.

Banks, D., Withers, J. G., Cashmore, G. & Dimelow, C. 2013. An overview of the results of 61 in situ thermal response tests in the UK. . *Quarterly Journal of Engineering Geology and Hydrogeology*, **46**, 281-291.

Bertermann, D., Klug, H., Morper-Busch, L. & Bialas, C. Modelling vSGPs (very shallow geothermal potentials) in selected CSAs (case study areas). 2014. *Energy*, **71**, 226-244.

Bilskie, J. R., Horton, R. & Bristow, K. L. 1998. Test of a dual-probe heat-pulse method for determining thermal properties of porous materials. *Soil Science*, **163**, 346–355.

Bristow, K. L., Campbell, G. S. & Calissendorff, C. 1993. Test of a heat-pulse probe for measuring changes in soil water content. *Journal of the American Soil Science Society*, **57**, 930–934

Campbell, G. S., Calissendorff, C. & Williams, J.H. 1991. Probe for measuring soil specific heat using a heat pulse method. *Journal of the American Soil Science Society*, **55**, 291–293.

Clarke, B. G., Agab, A. & Nicholson, D. 2008. Model specification to determine thermal conductivity of soils. *Proceedings of the Institution of Civil Engineers Geotechnical Engineering*, **161**, 161-168.

Curtis, R., Pine, T. & Wickins, C. 2013. Development of new ground loop sizing tools for domestic GSHP installations in the UK. European Geothermal Congress 2013, Pisa, Italy, 3-7 June, 10 pp.

Dehner, U. 2007. Bestimmung der thermischen Eigen-schaften von Böden als Grundlage für die Erdwärmenutzung. *Mainzer geowissenschaftliche Mitteilungen*, **35**, Mainz, 159-186.

Dingman, S. L. 2002. Physical Hydrology. 2nd Edition. Prentice Hall.

Gao, Z. Wang, L. & Horton, R. 2009. Comparison of six algorithms to determine the soil thermal diffusivity at a site in the Loess Plateau of China. *Hydrology and Earth System Sciences Discussions*, **6**, 2247-2274.

Gonzaez, R. Q., Verhoef, A., Vidale, P. L., Main, B. & Gan, G. 2012. Interactions between the physical soil environment and a horizontal ground coupled heat pump, for a domestic site in the UK. *Renewable Energy*, **44**, 141-153.

GSHPA. 2014. Shallow Ground Source Standard, Issue 1.0, July 2014. Ground Source Heat Pump Association.

Hinkel, K. M. 1997. Estimating seasonal values of thermal diffusivity in thawed and frozen soils using temperature time series. *Cold Regions Science and Technology*, **26**, 1-15.

Hodgson, J. M. 1997. Soil Survey field Handbook: Describing and sampling soil profiles. Soil Survey Technical Monograph No. 5, Third edition. Soil Survey and Land Research Centre, Silsoe, England.

Horton, R., Wierenga, P. J. & Nielsen, D. R. 1983. Evaluation of methods for determining apparent thermal diffusivity of soil near the surface, *Journal of the American Soil Science Society*, **47**, 23–32.

IAEA. 2008. Field estimation of soil water content. A practical guide to methods, instrumentation and sensor technology. International Atomic Energy Agency, Training Course Series 30, Vienna.

IGSHPA. 1989. Soil and Rock Classification for the Design of Ground-Coupled Heat Pump Systems: Field Manual. Oklahoma State University: International Ground Source Heat Pump Association Publications.

IGSHPA. 1996. Closed-loop/Ground-Source Heat Pump Systems: Installation guide. Oklahoma State University: International Ground Source Heat Pump Association Publications.

Kappelmeyer, O. & Haenel, R. 1974. Geothermics with special reference to application. Geoexploration Monographs Series 1 – No 4, Gebruder Borntraeger: Berlin - Stuttgart 238 pp.

Kersten, M. S. 1949. Thermal Properties of Soil. University of Minnesota, Engineering Experiment Station, *Bulletin 28,* Minneapolis, 227 pp.

King, W., Banks, D. & Findlay, J. 2012. Field determination of shallow soil thermal conductivity using a short-duration needle probe test. *Quarterly Journal of Engineering Geology and Hydrogeology*, **45**, 497-504.

Koo, M-H., Kim, Y., Suh, M. C. & Suh, M. S. 2003. Estimating thermal diffusivity of soils in Korea using temperature time series data. *Journal of the geological Society of Korea*, **39**, 301-317.

Koo, M-H. & Song, Y. 2008. Estimating apparent thermal diffusivity using temperatures time series: A comparison of temperature data measured in KMA boreholes and NGMN wells. *Geosciences Journal*, **12**, 255-264.

Lawley, R. 2008. The soil-parent material database: A user guide. *British Geological Survey Open Report* OR/08/034, 53 pp.

Met Office. 2010. Observations. National Meteorological Library and Archive Fact Sheet 17 – Weather observations over land. www.metoffice.gov.uk/media/pdf/k/5/Fact_sheet_No._17.pdf.

Preene, M. & Powrie, W. 2009. Ground energy systems: from analysis to geotechnical design. *Géotechnique*, **59**, 261-271.

Saxton, K. E., Rawls, W. J., Romberger, J. S. & Papendick, R. I. 1986. Estimating generalised soil-water characteristics from texture. *Journal of the American Soil Science Society*, **50**, 1031-1036.

VDI. 2001. Thermal use of the underground: Ground source heat pump systems. Verein Deutscher Ingenieure. Richtlinien VDI 4640 Blatt2/Part2 , September 2001, Düsseldorf, 43 pp.

Verhoef, A., van den Hurk, B. J., Jacobs, J. M., & Heusinkveld, A. F. G. 1996. Thermal soil properties for a vineyard (EFEDA-I) and a savanna (HAPEX-Sahel) sites, *Agricultural and Forest Meteorology*, **78**, 1–18.

Waples, D. W. & Waples, J. S. 2004a. A review and evaluation of specific heat capacities of rocks, minerals and subsurface fluids. Part 1: Minerals and nonporous rocks. *Natural Resources Research*, **13**, 97-122.

WAPLES, D. W. & WAPLES, J. S. 2004b. A review and evaluation of specific heat capacities of rocks, minerals and subsurface fluids. Part 2: Fluids and porous rocks. *Natural Resources Research*, **13**, 123-130.

Figures

Figure 1. The 65 UK Met Office stations from which soil temperature data have been used. The stations are identified by their station numbers (src_id) which can be cross referenced with the station names and geographical data in Table 1.

Figure 2. Temperature records for 3 years at 30 cm (black lines) and 100 cm (grey lines) depths from the UK meteorological station at Woburn (src_id = 458). Erratic lines are the daily measurements and the smooth lines are the best fit of an appropriate periodic function. The amplitudes, A_1 and A_2, of the two series are shown along with the phase shift, δt, between the series.

Figure 3. Plot of the amplitude damping versus the phase delay for all 73 thermal diffusivity determinations. The bold line is a plot of $\ln(A_2/A_1) = -\omega\delta t$, along which heat transfer is solely by one-dimensional conductive flow, whilst the two dashed lines are a deviation from this equation by ± 4%. Points that plot between the dashed lines have been taken as being representative of one dimensional conductive heat transfer.

Figure 4. Thermal diffusivities, derived as the mean of accepted amplitude and phase determinations, plotted against the dominant soil types as a box-whisker plot. The box extent is defined by the lower and upper quartiles and the line within the box is the median. The caps at the end of each box are the minimum and maximum values.

Figure 5. Estimated thermal conductivities plotted against the dominant soil types as a box-whisker plot. The box extent is defined by the lower and upper quartiles and the line within the box is the median. The caps at the end of each box are the minimum and maximum values.

Figure 6. Plot of estimated thermal conductivities derived from the soil temperature measurements against those derived by the methodology of Bertermann et al. (2014). The solid line is the line of a perfect positive fit between the two data sets where the correlation coefficient = +1.

Tables

Table 1. UK Met Office weather stations from which soil temperature data was used. The unique source identifier (src_id) is the Met Office weather station number, eastings and northings are British National Grid and elevation is relative to OD (Ordnance Datum).The depth range refers to the depth below ground level of the two temperature measurements from which the thermal diffusivity was derived.

Table 2. Thermal diffusivities, derived as the mean of accepted amplitude and phase determinations, soil texture from Lawley (2008) and estimated parameters based on the soil texture. The estimated thermal conductivity, derived from the diffusivity and the estimated parameters, is shown in the last column.

Table 3. Description of the soil texture classes, after Lawley (2008).

Table 4. Comparison of specific heat capacities, S_c, from those estimated in this study to measurements by Adjepong (1997).

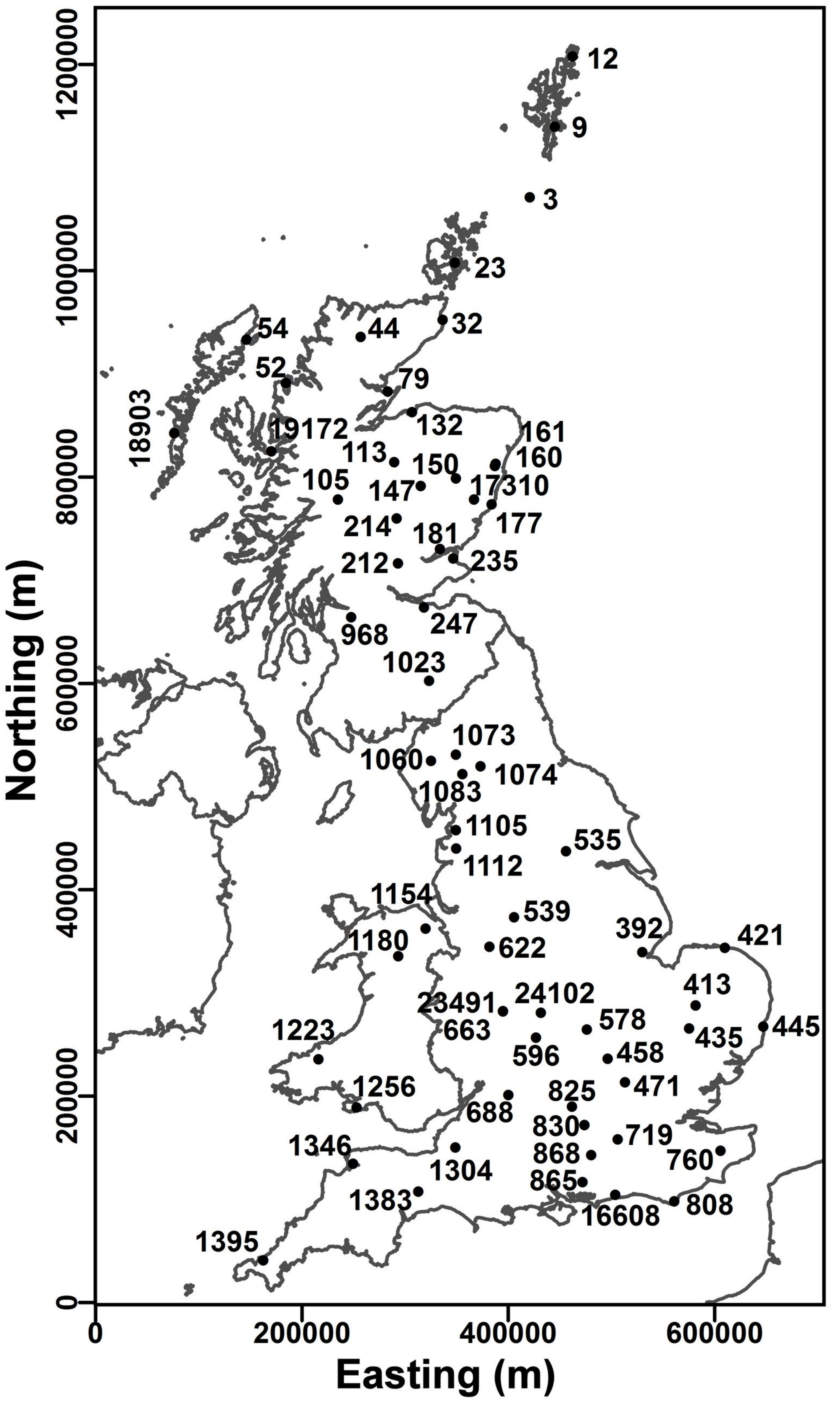

Northing (m)
Easting (m)
0
200000
400000
600000
800000
1000000
1200000
12
9
3
23
32
54
44
52
79
132
18903
19172
161
113
150
160
105
147
17310
214
177
181
212
235
968
247
1023
1073
1060
1074
1083
1105
535
1112
1154
539
392
421
1180
622
413
23491
24102
663
578
445
1223
596
435
458
471
1256
825
688
830
719
1346
868
760
1304
865
1383
16608
808
1395

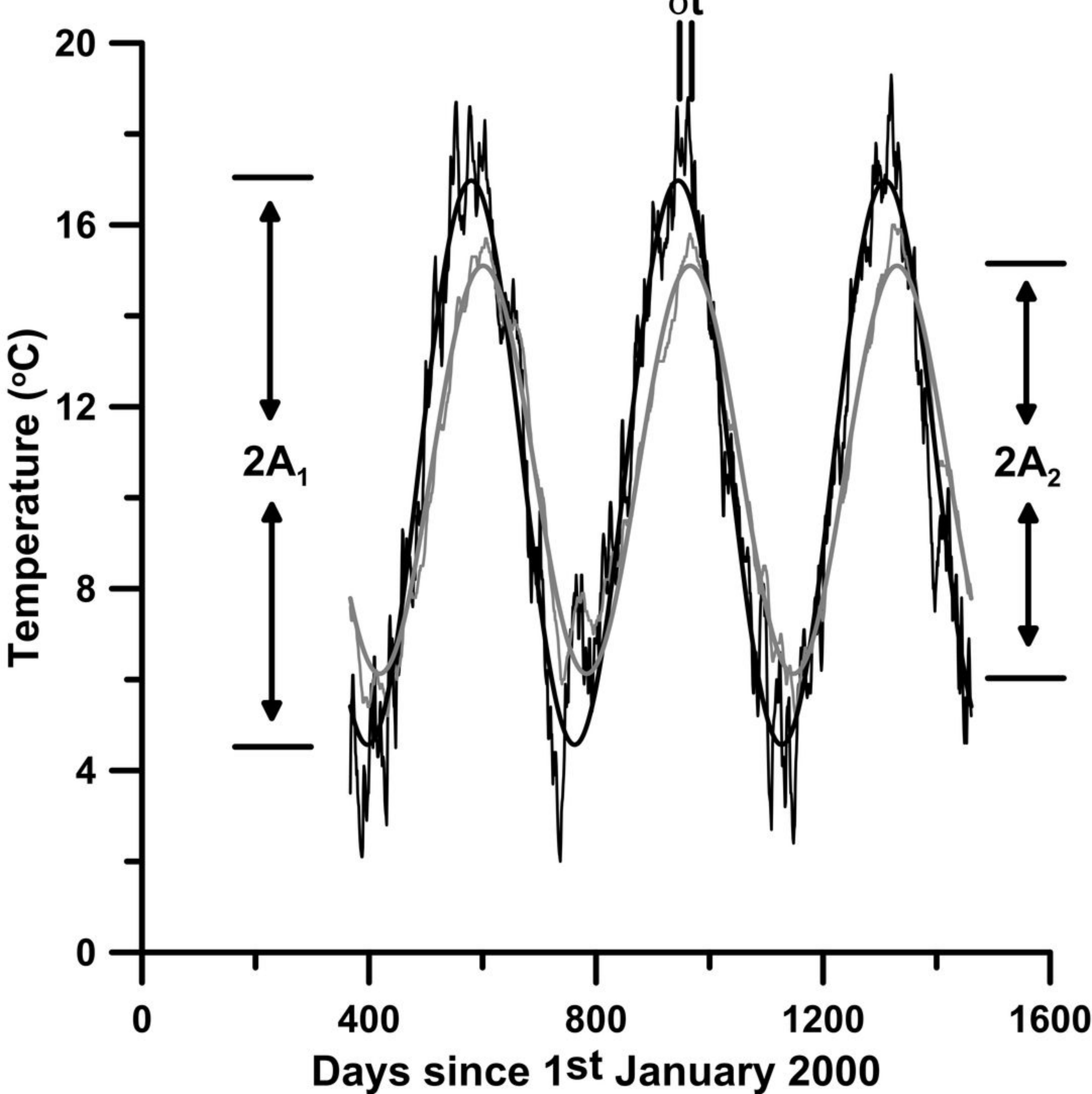

δt
20
16
12
8
4
0
Temperature (°C)
2A1
2A2
0
400
800
1200
1600
Days since 1st January 2000

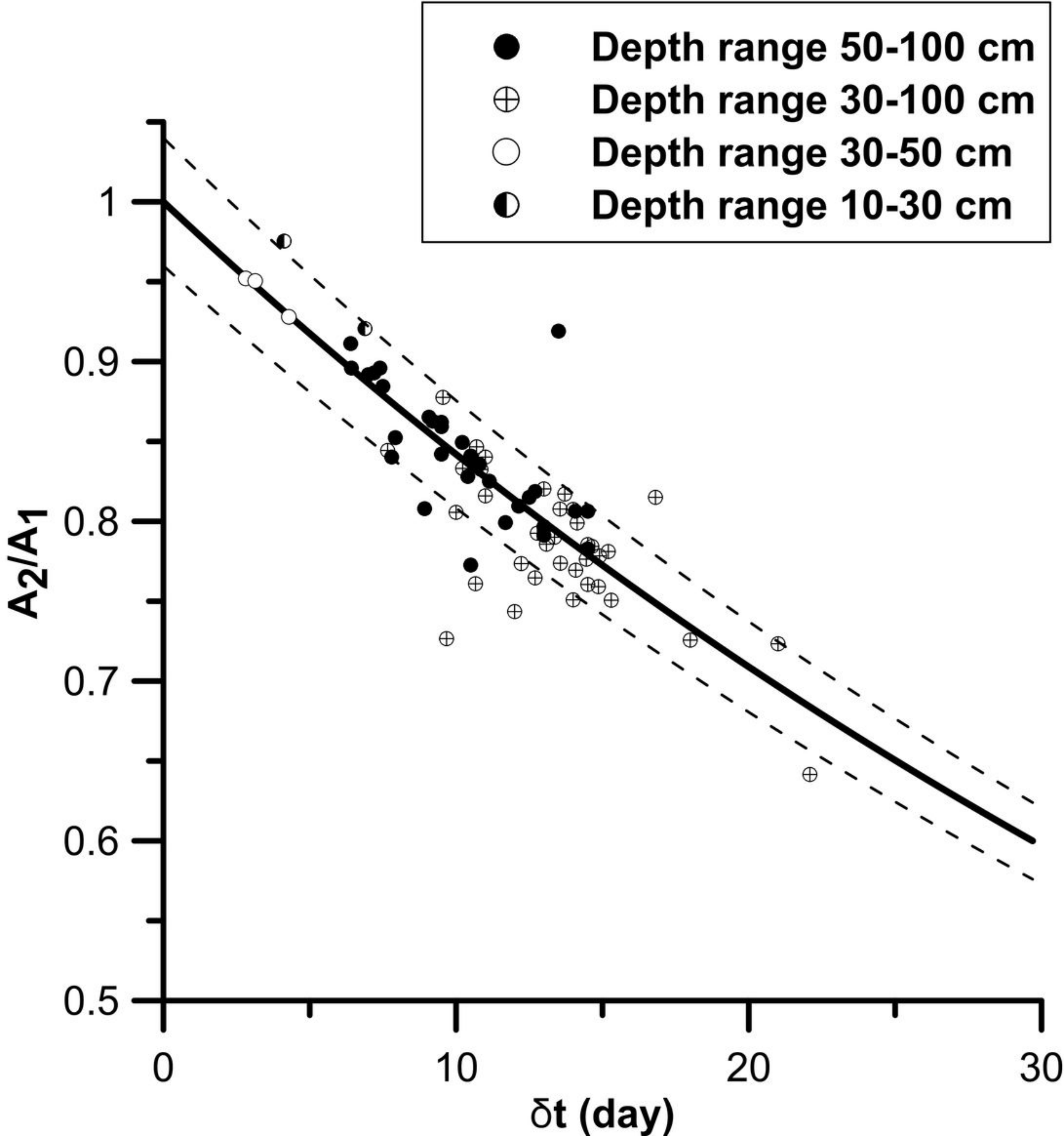

Depth range 50-100 cm
Depth range 30-100 cm
Depth range 30-50 cm
Depth range 10-30 cm
1
0.9
0.8
0.7
0.6
0.5
A_2/A_1
0
10
20
30
δt (day)

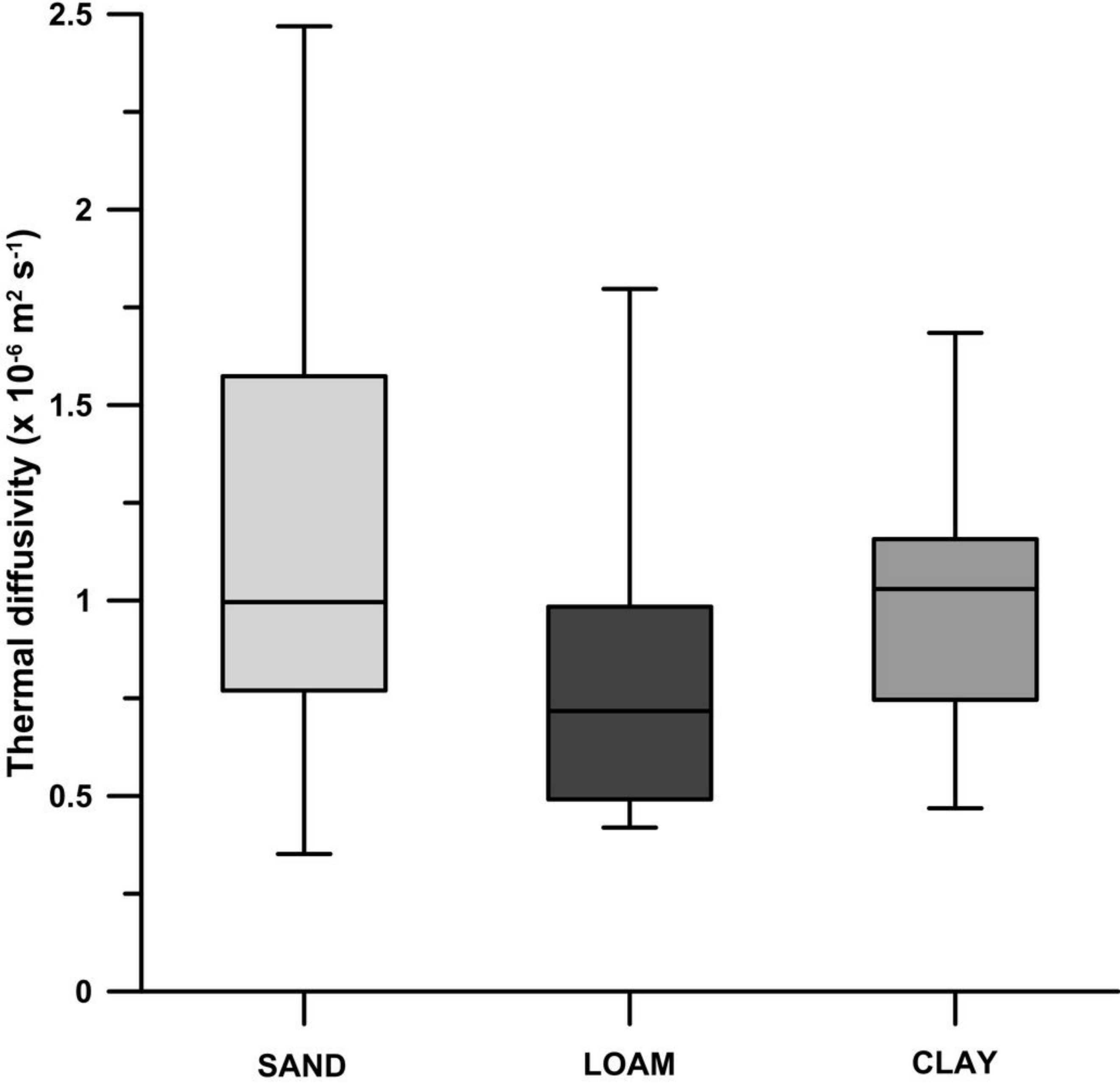
2.5
2
1.5
1
0.5
0
Thermal diffusivity (x 10^{-6} m^2 s^{-1})
SAND
LOAM
CLAY

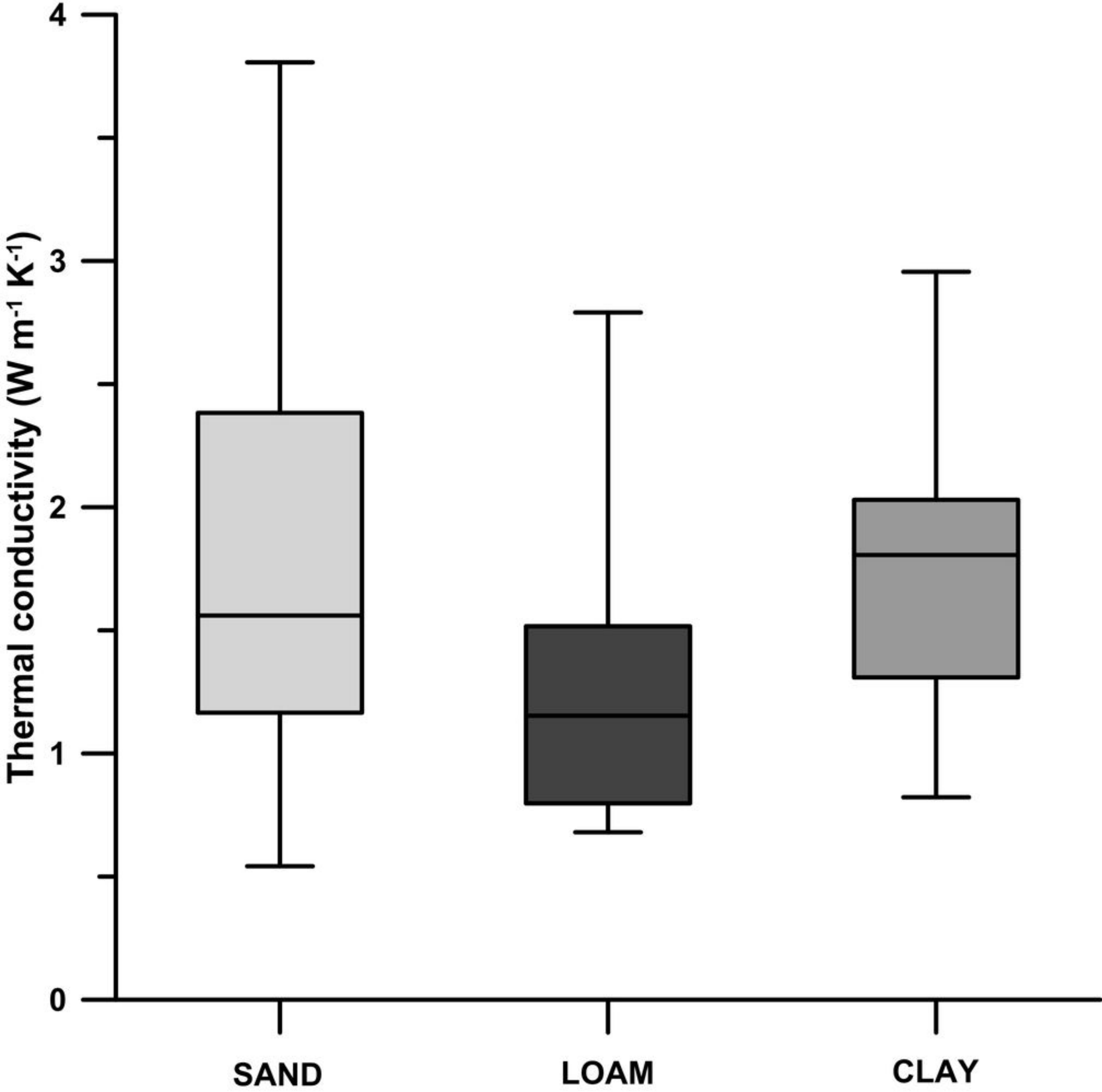

Thermal conductivity (W m-1 K-1)
4
3
2
1
0
SAND
LOAM
CLAY

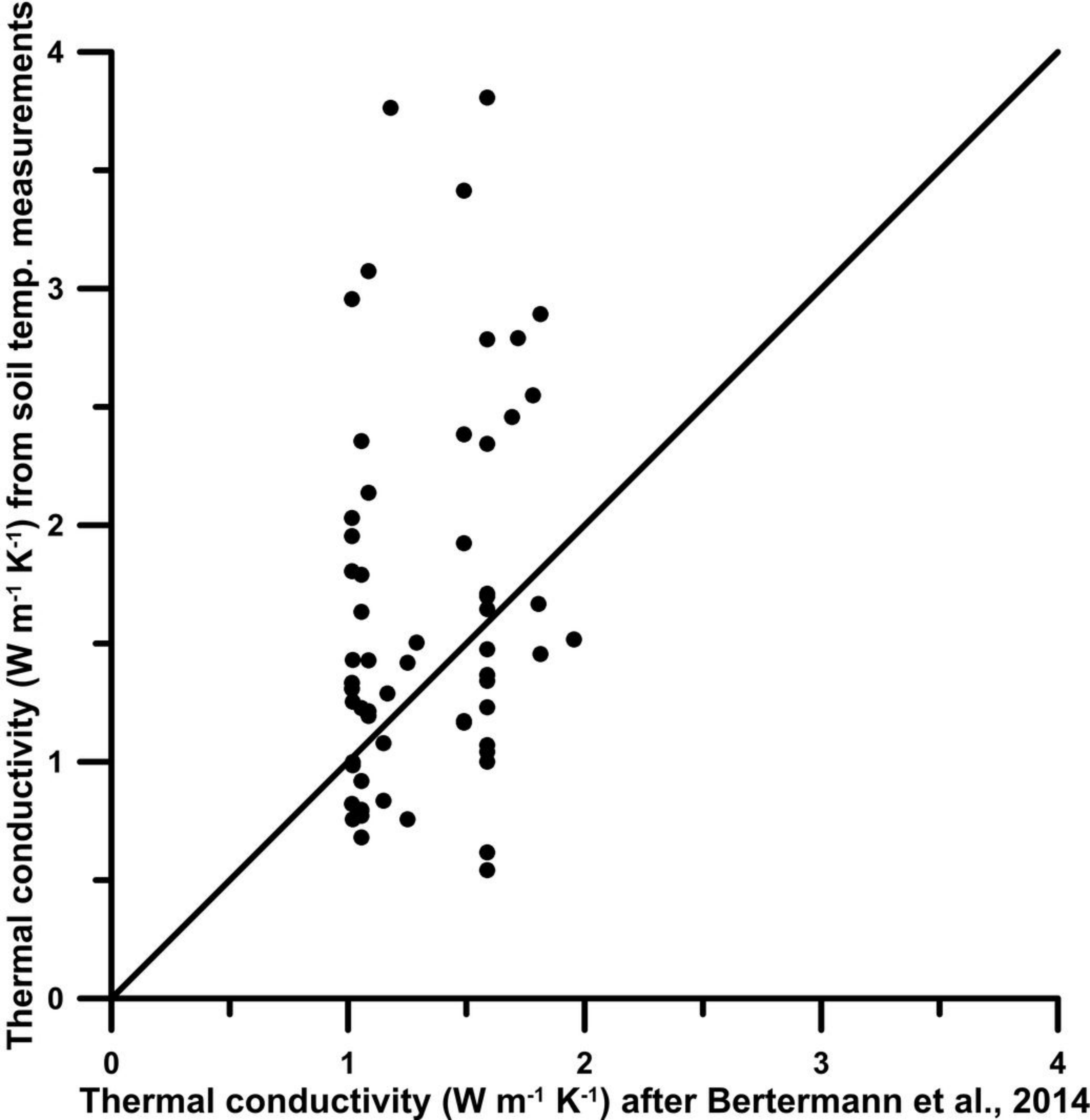

Thermal conductivity (W m-1 K-1) from soil temp. measurements
Thermal conductivity (W m-1 K-1) after Bertermann et al., 2014
0
1
2
3
4

Table 1

Src_id	Met Office station name	Easting (m)	Northing (m)	Elevation (mAOD)	Depth range (cm)
3	Fair Isle	421046	1071185	57	30-100
9	Lerwick	445392	1139664	82	30-100
12	Baltasound No 2	462488	1207786	15	10-30
32	Wick Airport	336490	952230	36	10-30
23	Kirkwall	348236	1007709	26	30-100
44	Altnaharra No 2	256908	935830	81	30-100
52	Aultbea No 2	184575	891274	11	30-100
54	Stornoway Airport	146443	933104	15	30-100
79	Tain Range	283272	882720	4	30-100
105	Tulloch Bridge	235030	778298	237	30-100
113	Aviemore	289652	814315	228	30-100
132	Kinloss	306774	862804	5	30-100
147	Braemar	315200	791400	339	50-100
150	Aboyne No 2	349300	798700	140	30-100
160	Craibstone	387100	810700	102	30-100
161	Dyce	387810	812800	65	30-100
177	Inverbervie No 2	383884	773425	134	30-100
181	Mylnefield	333900	730100	31	50-100 & 30-100
212	Strathallan airfield	293100	716200	35	30-100
214	Faskally	291800	759900	94	30-100
235	Leuchars	346800	720900	10	30-100
247	Edinburgh, East Craigs	318500	673500	61	30-50
392	Kirton Horticulture	529920	339450	4	50-100
413	Santon Downham	581600	287900	6	50-100 & 30-100
421	Weybourne	609900	343700	21	30-100
435	Brooms Barn	575300	265600	75	50-100
445	Westleton	647300	267200	10	50-100
458	Woburn	496400	236000	89	30-100
471	Rothamsted	513156	213280	128	50-100 & 30-100
535	Cawood	456100	437200	6	50-100
539	Buxton	405800	373400	307	50-100 & 30-100
578	Northampton, Moulton Park	476400	264500	127	50-100 & 30-100
596	Wellesbourne	427100	256500	47	50-100
622	Keele	381900	344600	179	50-100
663	Halesowen	394900	282200	153	50-100
688	Cirencester	400300	201100	133	30-50
719	Wisley	506300	157900	38	50-100
760	Wye	605890	147010	56	50-100
808	Eastbourne	561100	98000	7	30-100
825	Wallingford	461800	189800	48	50-100 & 30-100
830	Reading University, Whiteknights No 3	473900	171900	66	50-100
865	Butser, Windmill Hill	472000	116500	92	50-100
868	Alice Holt Lodge	480500	142700	115	50-100
968	Paisley	247895	664032	32	50-100
1023	Eskdalemuir	323500	602600	242	30-100
1060	Keswick	325300	524900	81	30-100
1073	Newton Rigg	349300	530800	169	30-50
1074	Warcop Range	373300	519700	227	30-100
1083	Shap	355700	512000	255	30-100
1105	Hazelrigg	349300	457820	95	50-100
1112	Myerscough	349500	440000	14	50-100
1154	Loggerheads, Colomendy Centre	320030	362160	210	50-100
1180	Bala	293500	335600	163	50-100
1223	Whitechurch	216200	235600	129	50-100
1256	Penmaen	253100	188800	87	50-100
1304	Rodney Stoke	348849	150155	40	50-100
1346	Chivenor	249600	134400	6	30-100
1383	Dunkeswell Aerodrome	312815	107480	252	30-100
1395	Camborne	162700	40700	87	30-100
16608	Littlehampton, Toddington Lane	503700	104100	3	50-100
17310	Fettercairn, Glensaugh No 2	366900	778200	171	30-100
18903	South Uist range	76312	842502	4	30-100
19172	Skye: Lusa	170593	824888	18	30-100
23491	Halesowen No 2	394900	282100	153	50-100 & 30-100
24102	Coventry, Coundon	431600	280800	119	50-100 & 30-100

Table 2

Src_id	Abbreviated station name	Depth range (cm)	Thermal diffusivity ($x10^{-6}$ m^2 s^{-1})	Soil texture	Bulk density (g cm^{-3})	Particle density (g cm^{-3})	Porosity	Volumetric moisture content	Specific heat (J kg^{-1} K^{-1})	Thermal conductivity (W m^{-1} K^{-1})
3	Fair Isle	30-100	0.9003	L	1.43	2.47	0.42	0.10	1102	1.42
32	Wick Airport	10-30	0.4331	XCL_C	1.25	2.60	0.52	0.18	1398	0.76
23	Kirkwall	30-100	0.8190	XCL_C	1.25	2.60	0.52	0.18	1398	1.43
44	Altnaharra No 2	30-100	0.9568	S_NL	1.52	2.62	0.42	0.08	1014	1.48
52	Aultbea No 2	30-100	0.7698	S_L	1.47	2.53	0.42	0.08	1030	1.17
54	Stornoway Airport	30-100	0.9537	L_C_S	1.31	2.34	0.44	0.10	1144	1.43
105	Tulloch Bridge	30-100	1.5996	S_SZL	1.61	2.78	0.42	0.08	990	2.55
113	Aviemore	30-100	0.8963	S_LS	1.66	2.86	0.42	0.08	978	1.45
132	Kinloss	30-100	0.7746	S_L	1.47	2.53	0.42	0.08	1030	1.17
147	Braemar	50-100	1.0672	S_SXL	1.52	2.62	0.42	0.08	1014	1.65
150	Aboyne No 2	30-100	1.0354	S_SL	1.62	2.70	0.40	0.08	994	1.67
160	Craibstone	30-100	1.1091	S_NL	1.52	2.62	0.42	0.08	1014	1.71
161	Dyce	30-100	0.6938	S_NL	1.52	2.62	0.42	0.08	1014	1.07
177	Inverbervie No 2	30-100	0.7979	S_NL	1.52	2.62	0.42	0.08	1014	1.23
181	Mylnefield	50-100	0.4002	S_NL	1.52	2.62	0.42	0.08	1014	0.62
		30-100	0.3517							0.54
235	Leuchars	30-100	2.2544	S_L	1.47	2.53	0.42	0.08	1030	3.41
247	Edinburgh	30-50	0.7175	C_S	1.32	2.36	0.44	0.10	1139	1.08
392	Kirton	50-100	0.7461	ML_C	1.24	2.48	0.50	0.18	1415	1.31
413	Santon Downham	50-100	1.1016	S_NL	1.52	2.62	0.42	0.08	1014	1.70
421	Weybourne	30-100	1.4861	S_XZL	1.57	2.71	0.42	0.10	1053	2.46
435	Brooms Barn	50-100	1.1036	L_C	1.28	2.46	0.48	0.14	1267	1.79
445	Westleton	50-100	1.7815	S_LS	1.66	2.86	0.42	0.08	978	2.89
458	Woburn	30-100	0.4193	L_C	1.28	2.46	0.48	0.14	1267	0.68
471	Rothamsted	50-100	0.4687	ML_C	1.24	2.48	0.50	0.18	1415	0.82
		30-100	0.7600							1.33
535	Cawood	50-100	1.5739	S_L	1.47	2.53	0.42	0.08	1030	2.38
539	Buxton	50-100	1.1571	ML_C	1.24	2.48	0.50	0.18	1415	2.03
		30-100	1.1136							1.95
578	Northampton	30-100	0.7172	XCL_C	1.25	2.60	0.52	0.18	1398	1.25
596	Wellesbourne	50-100	1.7971	NL	1.54	2.66	0.42	0.08	1008	2.79
622	Keele	50-100	0.5663	L_C	1.28	2.46	0.48	0.14	1267	0.92
663	Halesowen	50-100	0.4894	L_C	1.28	2.46	0.48	0.14	1267	0.79
688	Cirencester	30-50	1.6848	ML_C	1.24	2.48	0.50	0.18	1415	2.96
719	Wisley	50-100	0.8872	S_SXL	1.52	2.62	0.42	0.08	1014	1.37
760	Wye	50-100	1.0071	L_C	1.28	2.46	0.48	0.14	1267	1.63
808	Eastbourne	30-100	0.7568	L_C	1.28	2.46	0.48	0.14	1267	1.23
825	Wallingford	50-100	0.6754	S_SXL	1.52	2.62	0.42	0.08	1014	1.04

Table 2

830	Reading	50-100	0.8700	S_SXL	1.52	2.62	0.42	0.08	1014	1.34
865	Butser	50-100	0.7385	ML_ZC	1.35	2.60	0.48	0.16	1292	1.29
868	Alice Holt Lodge	50-100	0.4808	L	1.43	2.47	0.42	0.10	1102	0.76
968	Paisley	50-100	0.5558	C_S	1.32	2.36	0.44	0.10	1139	0.84
1023	Eskdalemuir	30-100	0.9003	LS_SZL	1.64	2.93	0.44	0.10	1027	1.52
1073	Newton Rigg	30-50	1.4517	L_C	1.28	2.46	0.48	0.14	1267	2.35
1074	Warcop Range	30-100	1.5203	S_NL	1.52	2.62	0.42	0.08	1014	2.34
1083	Shap	30-100	0.8101	ALL	1.31	2.34	0.44	0.10	1144	1.21
1105	Hazelrigg	50-100	0.5641	XCL_C	1.25	2.60	0.52	0.18	1398	0.99
1112	Myerscough	50-100	0.7963	ALL	1.31	2.34	0.44	0.10	1144	1.19
1154	Loggerheads	50-100	1.0295	ML_C	1.24	2.48	0.50	0.18	1415	1.81
1180	Bala	50-100	2.0517	ALL	1.31	2.34	0.44	0.10	1144	3.07
1256	Penmaen	50-100	2.4691	S_NL	1.52	2.62	0.42	0.08	1014	3.81
1304	Rodney Stoke	50-100	0.5719	XCL_C	1.25	2.60	0.52	0.18	1398	1.00
1346	Chivenor	30-100	1.4258	ALL	1.31	2.34	0.44	0.10	1144	2.14
1395	Camborne	30-100	2.3343	L_ZC	1.38	2.51	0.45	0.12	1169	3.76
16608	Littlehampton	50-100	1.8061	S_SXL	1.52	2.62	0.42	0.08	1014	2.78
17310	Fettercairn	30-100	0.6487	S_NL	1.52	2.62	0.42	0.08	1014	1.00
18903	South Uist range	30-100	1.2710	S_L	1.47	2.53	0.42	0.08	1030	1.92
23491	Halesowen No 2	50-100	0.4757	L_C	1.28	2.46	0.48	0.14	1267	0.77
		30-100	0.4916							0.80
24102	Coventry	30-100	0.9842	L_S	1.47	2.45	0.40	0.08	1039	1.50

Table 3

Soil texture	Description	Soil texture	Description
ALL	ALL	ML_ZC	CLAYEY TO SILTY LOAMS (LIMITED SAND) TO SILTY CLAY
C_S	CLAY, SAND, SANDY LOAMS, BUT GENERALLY LESS THAN 40% SILT)	NL	SANDY, CLAYEY AND SILTY LOAMS (MINIMUM 20%SAND)
CL_ZCL	CLAY LOAM TO SILTY CLAY LOAM	S_L	SANDY AND LOAMY SOILS (LIMITED CLAY)
L	LOAMY SOILS (ALL TYPES)	S_LS	SANDY TO LOAMY SAND
L_C	LOAM TO CLAY	S_NL	SAND TO SANDY, CLAYEY AND SILTY LOAMS
L_C_S	LOAM TO CLAY TO SAND	S_SL	SANDY TO SANDY- LOAM SOIL
L_S	LOAM TO SAND	S_SXL	SANDY TO SANDY- LOAM AND SANDY CLAY LOAM
L_ZC	LOAM TO SILTY CLAY	S_XZL	SANDY AND SANDY-SILTY LOAMS (LITTLE CLAY)
LS_SZL	LOAMY SAND TO SANDY SILT LOAM	S_SZL	SAND TO SANDY SILT LOAM
ML_C	CLAYEY TO SILTY LOAMS (LIMITED SAND) TO CLAY	XCL_C	SANDY CLAY, CLAY AND SILTY CLAY LOAM TO CLAY

Table 4

Soil texture	**Moisture content %**	**S_c (J kg^{-1} K^{-1}) from Adjepong (1997)**	**Estimated S_c (J kg^{-1} K^{-1}) (Averages from Table 2)**
Clay	16	1500	1415
Sandy loam	8	900	1014
Sand	8	900	986